INTERNATIONAL JOURNAL OF ADAPTIVE CONTROL AND SIGNAL PROCESSING
Int. J. Adapt. Control Signal Process. (2008)
Published online in Wiley InterScience (www.interscience.wiley.com). DOI: 10.1002/acs.1038

Robust fault detection using zonotope-based set-membership consistency test

Ari Ingimundarson[1,*,†], José Manuel Bravo[2], Vicenç Puig[1], Teodoro Alamo[3] and Pedro Guerra[1]

[1]*Departament d'Enginyeria de Sistemes, Automàtica i Informàtica Industrial, Campus de Terrassa, Universitat Politècnica de Catalunya, Rambla Sant Nebridi, 10, 08222 Terrassa, Spain*
[2]*Departamento de Ingeniería Electrónica, Sistemas Informáticos y Automática, Universidad de Huelva, Carretera Huelva-La Rábida, Palos de la Frontera, 21071 Huelva, Spain*
[3]*Departamento de Ingeniería de Sistemas y Automática, Universidad de Sevilla Escuela Superior de Ingenieros, Camino de los Descubrimientos s/n, 41092 Sevilla, Spain*

SUMMARY

This article proposes a robust fault detection method that takes advantage of a recently proposed set-membership identification procedure based on zonotopes for systems linear in the parameters. It is shown that consistency checks indicating faults can be performed in a natural manner with a zonotope description of the feasible parameter set. A zonotope-based fault detection algorithm that is able to handle systems with invariant parameters, with parameter variation bounded between samples and with unbounded variation is presented. Finally, two application examples are given, which demonstrate how the algorithm works on a simulated process (a four-tank system) and a real application example (a section of a sewer network).

Received 8 September 2006; Revised 5 February 2008; Accepted 8 February 2008

KEY WORDS: fault detection; set-membership identification; robustness

1. INTRODUCTION

Model-based fault detection is based on the use of mathematical models of the monitored system. Reliability and performance of fault detection algorithms depend on the quality of the model used.

*Correspondence to: Ari Ingimundarson, Departament d'Enginyeria de Sistemes, Automàtica i Informàtica Industrial, Campus de Terrassa, Universitat Politècnica de Catalunya, Rambla Sant Nebridi, 10, 08222 Terrassa, Spain.
†E-mail: ari.ingimundarson@upc.edu

Contract/grant sponsor: Research Commission of the Generalitat of Catalunya; contract/grant number: 2005SGR00537
Contract/grant sponsor: Spanish Ministry of Science and Technology; contract/grant numbers: DPI-2005-05415, DPI2006-15476-C02-01, DPI2007-66718-C04-01

These algorithms can often be improved by refining the models they are based on. However, high fidelity models are costly and modeling errors and disturbances in complex engineering systems are inevitable. Hence, there is a need to develop robust fault detection algorithms where model uncertainty is explicitly taken into account. The robustness of a fault detection system indicates its ability to distinguish between faults on the one hand and model uncertainty and disturbances on the other hand, see [1].

The robust fault detection research has roughly focused on two distinct approaches. In one of the approaches, characterized as active, the central idea is to decouple the effect of the uncertainty [1]. The other approach, known as passive, is based on enhancing the robustness of the fault detection system at the decision-making stage [2]. The aim with the passive approach is usually to determine, given a set of models, whether there is any member in the set that can explain the measurements. A common way to address this problem is to propagate the model uncertainty to the alarm limits of the residuals. When the residuals are outside the alarm limits, it is argued that model uncertainty alone cannot explain the residual and therefore a fault must have occurred, see [3] for a recent article using this approach and [4] for a survey of these techniques. A drawback of these techniques is that faults that produce a residual deviation smaller than the residual uncertainty due to parameter uncertainty will not be detected.

Another approach to the passive robust fault detection problem is to explicitly calculate the set of parameters that are consistent with the measurements [5]. When a measurement is found to be inconsistent with this set, a fault is assumed to have occurred. As an exact representation of the set of parameters consistent with the measurements is hard to calculate, outer bounds are often used instead, using algorithms coming from set-membership identification. This is the approach adopted in this article.

Set-membership identification methods have been the subject of a number of publications. They can be classified according to how the approximation of the feasible set of parameters is represented or parameterized. In [6], the set was overbounded by an ellipsoid. Other authors have focused on orthotopic approximations, see [7]. When using set-membership identification there is a trade-off between the set size (conservativeness) and the complexity of the identification method. Simpler methods generally lead to more conservative set estimates. In [8], it was claimed that parallelotopic estimates may be consistently better than ellipsoidal estimates while complexity is similar.

Other authors have used set-membership algorithms applied to fault detection, for example, see [9]. There, the feasible parameter set was approximated with an ellipsoid. A numerically robust ellipsoid state estimation algorithm was presented in [10]. In [11], a fault detection scheme based on orthotopic sets was presented. In [12], a consistency state-estimation-based fault detection scheme was presented, which uses the recursive optimal bounding parallelotope (ROBP) algorithm presented in [13]. They proposed a moving horizon strategy where an outer bound of the initial state was propagated using the ROBP and a fault was detected when no noise sequence within deterministic bounds could explain the observed data. Uncertainty in process parameters was not considered. In Figure 1, the distinct set of representations that have been used in the literature are shown.

In this article, the parameter set is bounded with zonotopes, which include parallelotopes as a special case. In [8], a set-membership identification algorithm was presented, which results in a parallelotopic representation of the parameter uncertainty for time-invariant systems. In [14], an extension of the previous algorithm based on zonotopes was presented to deal with time-variant systems. This article shows that the zonotope representation of the parameter uncertainty combined with the above-mentioned identification methods is particularly suitable for fault detection based

DOI: 10.1002/acs

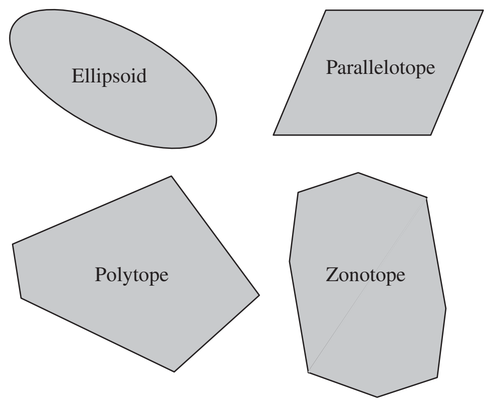

Figure 1. Distinct set of representations in the literature.

on consistency tests. Zonotopes provide better estimates of the parameter set leading directly to a better trade-off between false alarms and missed detections.

Zonotopes have appeared in set-membership approaches to fault detection before. In [15], an adaptive observer approach was presented where the residual evaluation was performed using set-membership computations based on zonotopes. In [16], parity relations were designed for linear systems with additive and multiplicative uncertainty. Both the mentioned methods treat linear system even though the system matrices could be time-varying.

This article, on the other hand, considers directly the analytical redundancy relations resulting from any fault detection design methodology (either non-linear or linear). By definition, an analytical redundancy relation depends only on the input-output data and thus can be expressed as a regression equation. It has been demonstrated that all model-based fault detection methodologies are equivalent in the sense that they all result in analytical redundancy relations dependent on input–output data [17]. Then, a typical starting point for the current methodology would be an analytical redundancy relation in regressor form that contains several uncertain parameters.

Only fault detection is considered in this article. Fault isolation is often performed by using a bank of residual relations, see [18, 19]. The focus of this article is a single residual relation that could form part of a larger diagnosis system.

The main contribution of this article is to present a robust fault detection algorithm for a regression equation that uses zonotope estimates of parameter uncertainty set and is based on the efficient algorithms presented in [14]. The algorithm is able to handle systems with invariant parameters, with parameter variation bounded between samples and with unbounded variation. Practical issues such as fault sensitivity are considered and guidelines on how to calibrate the algorithm are presented. As a remedy towards poor excitation in face of a possible parameter change, a heuristic version of the fault detection algorithm is proposed based on conditionally updating the parameter set when a variation has been detected. Finally, an application of the method to real data from limnimeters in a sewer network is presented.

This article is organized in the following manner. In Section 3, the problem of fault detection using a parameter consistency test is introduced and a conceptual algorithm is proposed. In Section 4, zonotopes and related operations required to implement the fault detection algorithm based on a parameter consistency test are introduced. In Section 5 practical issues are addressed

DOI: 10.1002/acs

such as characterizing the minimum detectable magnitude of abrupt sensor and parametric faults, how to calibrate the algorithm and the conditional updating approach is introduced. In Section 6, an example based on a four-tank system that allows one to show the fault detection performance in the case of invariant parameters and the time-varying case with unbounded and bounded variations is given. On the other hand, in Section 7, a real application based on a sewer network allows one to assess the case of bounded variation with conditional updating. Conclusions are presented in Section 8.

2. BACKGROUND AND NOTATION

In what follows, some preliminary notations are introduced. An interval $[a,b]$ is the set $\{x : a\leqslant x\leqslant b\}$. The unitary interval is $\mathbf{B}=[-1,1]$. A box is an interval vector. A unitary box in $\mathbb{R}^m$, denoted as $\mathbf{B}^m$, is a box composed of m unitary intervals. The Minkowski sum of two sets $\mathscr{X}$ and $\mathscr{Y}$ is defined by $\mathscr{X}\oplus\mathscr{Y}=\{x+y : x\in\mathscr{X}, y\in\mathscr{Y}\}$. Given a vector $p\in\mathbb{R}^n$ and a matrix $H\in\mathbb{R}^{n\times m}$, the set:

$$\mathscr{Z}=p\oplus H\mathbf{B}^m=\{p+Hz : z\in\mathbf{B}^m\}$$

is called a zonotope of order m. Note that this is the Minkowski sum of the segments defined by the columns of matrix H. A parallelotope is a zonotope with $n=m$. Given the parallelotope $\mathscr{P}=p\oplus H\mathbf{B}^n$, where $H\in\mathbb{R}^{n\times n}$ is invertible, $\mathscr{P}$ can be rewritten as $\mathscr{P}=\{x:\|H^{-1}x-H^{-1}p\|_\infty\leqslant 1\}$. The mathematical representation of an n-dimensional ellipsoid is $\mathscr{E}=\{x:(x-x_0)^{\mathrm{T}}H(x-x_0)\leqslant 1\}$ where $n\times n$ matrix H is positive definite. Finally, a polytope is a set that can be represented with linear inequalities, $\mathscr{P}=\{x:Ax\leqslant b\}$. Figure 1 shows the graphical representation of the zonotopes, polytopes, parallelotopes and ellipsoids.

3. MODEL-BASED DETECTION USING CONSISTENCY TESTS

3.1. Problem setup

The principle of *model-based detection using consistency tests* relies on checking whether the measured sequence of system inputs U and outputs Y available for N points, at every time instant k lies within the behavior described by a model of the faultless system [17]. If the measurements are inconsistent with the model of the faultless system, the existence of a fault is proved to conclude the fault detection task.

In this article it is assumed that the system output can be described by

$$y(k)=\varphi^{\mathrm{T}}(k)\theta(k)+e(k)+f_y(k) \tag{1}$$

$$\theta(k+1)=\theta(k)+w(k)+\theta_f(k) \tag{2}$$

$$\theta(0)\in\Theta \tag{3}$$

where $\theta(k)\in\mathbb{R}^n$ is the parameter vector whose values are assumed to be unknown but belong to a compact bounded initial set Θ, $\varphi(k)\in\mathbb{R}^n$ is the regressor vector that can contain any function of inputs and outputs, $f_y(k)$ is the sensor fault signal added to the regressor equation and $\theta_f(k)$ is the parametric fault signal, both are zero in the fault-free case. The noise $e(k)$ and parameter variation $w(k)$ are limited as

$$|e(k)|\leqslant\sigma \quad \text{and} \quad |w(k)|\leqslant\lambda \tag{4}$$

DOI: 10.1002/acs

As the parameter vector is assumed to belong to $\mathbb{R}^n$, so does λ and the last inequality is an elementwise inequality. Note that this system description includes any system linear in the parameters. Parameter uncertainty comes from physical modeling or from the set-membership parameter estimation algorithms applied in a non-faulty situation.

Note that Equation (2) specifies the allowed variance of uncertain parameters θ. Depending on the value of λ, three different cases can be considered

- time-invariant case, $\lambda=0$;
- bounded variance case 1, $\lambda=\bar{\lambda}$;
- unbounded variance case 2, $\lambda=\infty$.

In the first case, the parameter is unknown within Θ, but it is known that it will not vary. In the second case, the parameter variation is bounded specifically by a vector $\bar{\lambda}$, whereas in the last case, the variation is implicitly bounded only by the initial parameter set Θ and can vary at will within that set.

The first case represents situations when an initial variance comes from component specifications that are known only with a mean and variance in the beginning of the fault detection task. The second case represents a system that has been identified over a number of operation conditions, each with a different θ within Θ, but with the variance between samples bounded by $\bar{\lambda}$. The last case corresponds to systems whose sample-to-sample parameter variations are large enough such that the parameters can reach any value within the original parameter set.

A fourth case will also be considered in this article. A constant λ takes into account that systems can change continuously over time, for example, as they move from one operating region to another. If the system, on the other hand, does not move for an interval of time from a specific operating region, a constant λ can lead to conservativeness and poor fault sensitivity. This problem is specially difficult if there is poor excitation in the data set. As a remedy to this problem, a fault detection algorithm based on conditionally updating the parameter set depending on the severity of the inconsistency detected is used.

3.2. Fault detection algorithm

From the model description above the following sequences are defined:

$$\Phi_N=\{\varphi(k)\}_{k=0,\ldots,N-1}, \quad Y_N=\{y(k)\}_{k=0,\ldots,N-1} \tag{5}$$

To define what constitutes a fault, the feasible solution set at time N is defined as follows.

Definition 1

Given the data sequences Φ_N and Y_N, the parameter θ is said to belong to the *feasible solution set* at time N, (denoted FSS_k), if there exist $\theta(0), \theta(1), \ldots, \theta(N-1)$ such that

$$|y(k)-\varphi^{\mathrm{T}}(k)\theta(k)|\leqslant\sigma, \quad k=0,\ldots,N-1 \tag{6}$$

$$|\theta(k)-\theta(k-1)|\leqslant\lambda, \quad k=1,\ldots,N-1 \tag{7}$$

$$\theta(0)\in\Theta \tag{8}$$

Using the previous definition, a fault is now defined for the sequences Φ_N and Y_N.

Definition 2

Given the data sequences Φ_N and Y_N, a *fault* is said to have occurred if the set FSS_N is empty.

DOI: 10.1002/acs

Each new measurement defines a set of consistent parameters defined by

$$F_k = \{\theta \in \mathbb{R}^n : -\sigma \leqslant y(k) - \varphi(k)^{\mathrm{T}}\theta \leqslant \sigma\} \tag{9}$$

where F_k is the region between two hyperplanes. The normalized form of this strip is expressed as

$$\begin{aligned} F_k &= \left\{ \theta \in \mathbb{R}^n : \left| \frac{y(k)}{\sigma} - \frac{\varphi(k)}{\sigma}^{\mathrm{T}} \theta \right| \leqslant 1 \right\} \\ &= \{\theta \in \mathbb{R}^n : |d(k) - c(k)^{\mathrm{T}}\theta| \leqslant 1\} \end{aligned} \tag{10}$$

This strip F_k available at time k allows one to iteratively refine the feasible parameter set FSS_k

$$\mathrm{FSS}_{k+1} = \mathrm{FSS}_k \cap F_k \tag{11}$$

and to detect the presence of a fault if its intersection with the feasible parameter set FSS_k is empty

$$\mathrm{FSS}_k \cap F_k = \emptyset \tag{12}$$

In practice, the computation of FSS_k is difficult. The fault detection algorithm presented in this article is based on using a zonotope to upper bound the feasible solution set, creating an approximate feasible solution set denoted as AFSS_k that fulfills $\mathrm{FSS}_k \subseteq \mathrm{AFSS}_k$ and for which consistency is checked. In the case when $\lambda > 0$, the set AFSS_k is expanded to take the allowed parameter variance into account in the next sample. The expanded set is denoted as $\overline{\mathrm{AFSS}}_{k+1}$.

Algorithm 1 provides a general conceptual form of the suggested fault detection strategy based on the use of a parameter consistency test. The basic idea of this algorithm is as follows: at every time instant, input/output system measurements obtained from sensors are used to build the regressor $\varphi(k)$ and strip F_k according to Equations (5) and (10), respectively. Then, consistency between strip and the zonotope AFSS_k is checked. In case consistency is proved, the algorithm proceeds to refine the current zonotope by its intersection with the strip F_k and the resulting zonotope is

Algorithm 1. Fault detection using a parameter consistency test

$k \leftarrow 0$
$\overline{\mathrm{AFSS}}_k \leftarrow \Theta$
while $k < N$ **do**
  Obtain input–output data $\{u(k), y(k)\}$ at time instant k, build regressor $\varphi(k)$ and strip F_k according to Equations (5) and (10).
  if $\overline{\mathrm{AFSS}}_k \cap F_k = \emptyset$
  Indicate **fault** and estimate the parameter variation $\Delta\theta$ using Equation (22) in order to identify the faulty parameters and the size of change.
  else Calculate AFSS_k that fulfills $F_k \cap \overline{\mathrm{AFSS}}_k \subset \mathrm{AFSS}_k$ and
  Expand AFSS_k taking into account λ to obtain $\overline{\mathrm{AFSS}}_{k+1}$.
  endif
  $k \leftarrow k+1$
end while

DOI: 10.1002/acs

expanded by the allowed parameter variance λ. Otherwise, if an inconsistency is detected, a fault is considered to be present.

4. IMPLEMENTATION OF THE FAULT DETECTION ALGORITHM USING ZONOTOPES

In this article, zonotopes are used to bound the set of uncertain estimated sets and to implement Algorithm 1. In this section, zonotopes and their related operations required to implement this algorithm are introduced. Looking at Algorithm 1, these operations are

- checking the consistency of a zonotope with a strip (step 5);
- intersection between a zonotope and a strip (step 7);
- expansion of the parameter set taking into account $\lambda(k)$ (step 8).

4.1. Checking consistency of a zonotope with a strip

Given a new data point $\{y(k)\}$ at time instant k, regressor $\varphi(k)$ and strip F_k according to Equation (10) is built. Assuming that $\text{FSS}_k \subseteq \mathscr{X}$, where $\mathscr{X} = p \oplus HB^m$ is a zonotope, consistency can be assessed by checking if

$$\mathscr{X} \cap F_k = \emptyset \tag{13}$$

This check is very easy to perform using the following definition:

Definition 3
Given a zonotope $\mathscr{X} = p \oplus H\mathbf{B}^m$ and a vector c, the *zonotope support strip* is defined by $F_S = x : q_\mathrm{d} \leqslant c^\mathrm{T} x \leqslant q_\mathrm{u}$, where q_d and q_u satisfy

$$q_\mathrm{u} = \max_{x \in \mathscr{X}} c^\mathrm{T} x \quad \text{and} \quad q_\mathrm{d} = \min_{x \in \mathscr{X}} c^\mathrm{T} x \tag{14}$$

and can easily be calculated as

$$q_\mathrm{u} = c^\mathrm{T} p + \|H^\mathrm{T} c\|_1 \tag{15}$$

$$q_\mathrm{d} = c^\mathrm{T} p - \|H^\mathrm{T} c\|_1 \tag{16}$$

where $\|\cdot\|_1$ is the 1-norm of a vector.

Then, calculating the constants q_u and q_d, the intersection between $\mathscr{X}$ and F_k is empty if and only if $F_S \cap F_k = \emptyset$ or

$$q_\mathrm{u} < \frac{y(k)}{\sigma} - 1 \quad \text{or} \quad q_\mathrm{d} > \frac{y(k)}{\sigma} + 1 \tag{17}$$

This condition of inconsistency was reported in [8].

4.2. Intersection between a zonotope and a strip

Definition 4
Given a zonotope $\mathscr{X} = p \oplus H\mathbf{B}^m$ and a strip $F = x : q_a \leqslant c^\mathrm{T} x \leqslant q_b$, the *zonotope tight strip* is obtained by $\mathscr{S} = F \cap F_S$, where F_S is the zonotope support strip defined by c and $\mathscr{X}$.

DOI: 10.1002/acs

According to Bravo *et al.* [14], given the zonotope $\mathscr{Z} = p_k \oplus H\mathbf{B}^r$, the tight strip $\mathscr{S} = \{x \in \mathbb{R}^n : |c^{\mathrm{T}}x - d| \leqslant \sigma\}$ and vector $\alpha \in \mathbb{R}^n$, a family of zonotopes containing the intersection between the zonotope and the strip is given by

$$\mathscr{Z} \cap \mathscr{S} \subseteq v(j) \oplus T(j)\mathbf{B}^r \tag{18}$$

where

$$v(j) = \begin{cases} p + \left(\dfrac{d - c^{\mathrm{T}}p}{c^{\mathrm{T}}H_j}\right)H_j & \text{if } 1 \leqslant j \leqslant r \text{ and } c^{\mathrm{T}}H_j \neq 0 \\ p & \text{otherwise} \end{cases}$$

and

$$T(j) = \begin{cases} [T_1^j T_2^j \ldots T_r^j] & \text{if } 1 \leqslant j \leqslant r \text{ and } c^{\mathrm{T}}H_j \neq 0 \\ H_j & \text{otherwise} \end{cases}$$

with

$$T_i^j = \begin{cases} H_i - \left(\dfrac{c^{\mathrm{T}}H_i}{c^{\mathrm{T}}H_j}\right)H & \text{if } i \neq j \\ \left(\dfrac{\sigma}{c^{\mathrm{T}}H_j}\right)H_j & \text{if } i = j \end{cases}$$

There are $r+1$ possible choices of j to obtain a zonotope that bounds the intersection. An optimum integer $j^*, 0 \leqslant j^* \leqslant r$, can be obtained such that the volume of the outer-bounding zonotope is minimized, i.e.

$$j^* = \arg \min_{0 \leqslant j \leqslant r} \mathrm{Vol}(v(j) \oplus T(j)\mathbf{B}^r) \tag{19}$$

where $\mathrm{Vol}(\cdot)$ denotes the volume of the zonotope $v(j) \oplus T(j)\mathbf{B}^r$. In order to compute j^*, the method proposed in [14] is used.

4.3. Expansion of the parameter set

The initial value of the approximated feasible set $\overline{\mathrm{AFSS}_0}$ is a zonotope $\mathscr{Z}_0$ initialized with the initial parameter set Θ. What differentiates the algorithm for the three cases of allowed parameter variance is the update procedure in step 8 of Algorithm 1. In all cases, at each iteration of the algorithm, the zonotope $\mathscr{Z}_k$ is an outer bounding of the feasible solution set FSS_k.

4.3.1. Bounded variance case ($\lambda = \bar{\lambda}$). Note that in this case the bound on parameter variation given by Equation (2) can be expressed as

$$\theta(k+1) \in \theta(k) \oplus \Lambda\mathbf{B}^n \tag{20}$$

where Λ is a diagonal matrix with the elements equal to λ. One of the principal features of zonotopes is that the Minkowski sum of a box and a zonotope is another zonotope. Therefore, if at time k it is known that the parameter belongs to set $\mathscr{Z}_k = p \oplus H\mathbf{B}^m$ then using Equation (20)

DOI: 10.1002/acs

and taking into account Equation (2), the parameter set at time $k+1$ can be expressed as

$$\mathscr{Z}_{k+1} = p \oplus H\mathbf{B}^m \oplus \Lambda\mathbf{B}^n = p \oplus [H \ \ \Lambda]\mathbf{B}^{m+n}$$

4.3.2. Unbounded variance case ($\lambda=\infty$). In this case, as the parameters can vary at will within the initial parameter set Θ, the update procedure consists of taking the zonotope $\mathscr{Z}_{k+1}$ equal to the initial parameter set Θ.

4.3.3. Time-invariant case ($\lambda=0$). In this case, as $\lambda=0$, the procedure in step 8 of Algorithm 1 returns the set unchanged.

4.4. Calculating the parameter variation when inconsistency occurs

Given a strip

$$|c^{\mathrm{T}}\theta(k) - d| \leqslant 1$$

that does not intersect a zonotope $\mathscr{Z} = p \oplus H\mathbf{B}^m$, the shortest variation of the parameter vector $\Delta\theta$ from the zonotope to the strip can be easily calculated. Assume that $q_{\mathrm{u}} < d-1$, where q_{u} is the constant of the 'upper' supporting hyperplane. Then the point $\hat{\theta}$ in $\mathscr{Z}$ that is closest to the strip can be calculated as

$$\hat{\theta} = p + H^{\mathrm{T}}(e_i) \tag{21}$$

where $e_i = [\mathrm{sign}(h_1^{\mathrm{T}}c) \ \mathrm{sign}(h_2^{\mathrm{T}}c) \cdots \mathrm{sign}(h_m^{\mathrm{T}}c)]^{\mathrm{T}}$. It is assumed that $\mathrm{sign}(0)=0$. The problem is then reduced to calculating the projection of a point to a hyperplane. The error $\Delta\theta$ is easily calculated as

$$\Delta\theta = \frac{d-1-c^{\mathrm{T}}\hat{\theta}}{\|c\|^2} c \tag{22}$$

5. PRACTICAL ISSUES

In this section, a number of practical issues related to the proposed algorithm are addressed.

5.1. Characterization of algorithm fault sensitivity

An important characteristic of robust fault detection algorithms is the sensitivity towards faults. In this section, the minimum abrupt fault magnitude that is guaranteed to cause an alarm will be determined for the output sensor faults $f_y(k)$ and parametric faults $\theta_f(k)$.

5.1.1. Minimum sensor fault magnitude $f_y(k)$. A fault is detected if either consistency check given by Equation (17) fails. Without loss of generality, the minimum abrupt fault magnitude will be determined for the left inequality in Equation (17). It is assumed that $\theta(k) \in p \oplus H\mathbf{B}^n$ and $e(k) \in [-\sigma, \sigma]$ (see Equation (4)). Substituting q_{u} with Equation (15) and $y(k)$ with Equation (1), the following equation is obtained:

$$c^{\mathrm{T}}p + \|H^{\mathrm{T}}c\|_1 < c^{\mathrm{T}}\theta(k) + \frac{e(k)}{\sigma} + \frac{f_y(k)}{\sigma} - 1 \tag{23}$$

Note that the index k of c, H and p has been omitted for simplicity.

DOI: 10.1002/acs

Assuming the worst-case values of $\theta(k)$ and $e(k)$, i.e. minimizing the term $c^{\mathrm{T}}\theta(k)+(e(k)/\sigma)$, the condition on the magnitude of $f_y(k)$ is obtained as

$$2\|H^{\mathrm{T}}c\|_1+2<\frac{f_y(k)}{\sigma} \tag{24}$$

where $2\|H^{\mathrm{T}}c\|_1$ stands for the width of the zonotope H in the c direction and the integer 2 is the width of the band (2σ) as $f_y(k)$ is normalized by σ in the equation. The condition given in Equation (24) shows that in addition to measurements noise amplitude σ, the width of the zonotope in the direction of normalized regression vector c determines the sensitivity of the algorithm to detect abrupt sensor faults.

5.1.2. Minimum parametric fault magnitude $\theta_f(k)$. Analogously, the minimum abrupt parametric fault magnitude will be determined for the left inequality in Equation (17) by substituting Equation (15) for q_{u}, Equation (1) for $y(k)$ and Equation (2) for $\theta(k)$. This yields

$$c^{\mathrm{T}}p+\|H^{\mathrm{T}}c\|_1<c^{\mathrm{T}}(\theta(k-1)+w(k-1)+\theta_f(k-1))+\frac{e(k)}{\sigma}-1 \tag{25}$$

Taking the parametric variation bounds given in Equation (4) into account, the condition for inconsistency becomes

$$2\|H^{\mathrm{T}}c\|_1+2+\sum_{i=1}^{n}|c_i\lambda_i|<c^{\mathrm{T}}\theta_f(k) \tag{26}$$

This condition shows that if the parameter fault is in an orthogonal direction to the normalized regression vector, the fault will never be detected, independent on the magnitude of the fault. Thus, the direction of the regression vector is of importance. This requirement is similar to the requirements of persistent excitation in system identification. This is an already known issue when applying parameter estimation methods to fault detection [20].

5.2. Calibration of algorithm

As seen in the previous section, the fault sensitivity of the presented algorithm depends on, among other things, noise level σ and parameter variation λ. It is desirable that these are as small as possible to maximize fault sensitivity. The selection of these parameters of the algorithm is, on the other hand, a non-trivial problem. If selected too small, false alarms can occur, whereas if selected too large, faults can go undetected.

In Section 3, a discussion was presented relating the distinct cases of λ to the properties of the system under consideration. For example, σ can sometimes be related to the sensor accuracies of the signals in Equation (1). If no previous information about σ and λ is available, it is possible to obtain preliminary values by using sets of data without faults. It should be noted that σ can always be selected so that $\lambda=0$, i.e. it is always possible to select the noise level large enough so that the system can be considered time invariant. This selection might be useless due to little sensitivity towards faults and frequent missed detections. A selection of σ and λ is therefore a decision of a suitable trade-off between false alarms and missed detections. Algorithm 2 is used to obtain an initial value of λ given a value of σ.

DOI: 10.1002/acs

Algorithm 2. Estimation of λ given a value of σ.

$k \leftarrow 0$
$\lambda \leftarrow 0$
$\text{AFSS}_k \leftarrow \Theta$
while $k < N$ **do**
  Obtain input–output data $\{u(k), y(k)\}$ at time instant k, build regressor $\varphi(k)$ and strip F_k according to Equations (5) and (10).
  if $\text{AFSS}_k \cap F_k = \emptyset$ (an inconsistency is detected)
  $\lambda_k \leftarrow \Delta\theta$ where $\Delta\theta$ is calculated using Equation (22)
  Expand AFSS_k taking into account λ_k
  else Calculate AFSS_{k+1} that fulfills $F_k \cap \text{AFSS}_k \subset \text{AFSS}_{k+1}$
  end if
  $k \leftarrow k+1$
  $\lambda_k \leftarrow 0$
end while
$\lambda = \max\{\lambda_0, \lambda_1, \ldots, \lambda_{N-1}\}$ (i.e. the maximum value component wise over all parameter error vectors $\Delta\theta$ encountered in the data set)

These steps can provide with a first guess of parameter λ. Conservativeness can be reduced by reducing λ and testing again whether inconsistency is observed when the algorithm is run on fault-free data.

5.3. *Fault detection using conditional updating*

In the calibration procedure described in Algorithm 2, the zonotope was allowed to vary only when an inconsistency was detected. A similar idea can be used for fault detection procedure presented in Algorithm 1. Step 5 in this algorithm is then changed so that if an inconsistency is detected, the zonotope is expanded by λ. Then, the fault detection test is repeated. If inconsistency persists, a fault is indicated. Otherwise, the fault is not indicated and the fault detection algorithm proceeds with the next sample. In case no inconsistency is detected, the expansion of the zonotope is not performed. Thus, the name conditional updating of the zonotope for this procedure follows.

This approach has many advantages. First of all, the conservativeness related to having a fixed λ at each sample can be reduced. The zonotope is in this way allowed to change as long as the change is not so large. This might be a more accurate description of parameter variation when systems spend large amount of time at a similar operating region where the parameters do not change.

6. APPLICATION EXAMPLE 1: FOUR-TANK SYSTEM

A quadruple-tank process (see [21]) is proposed as a first application example to understand how the fault detection algorithm proposed in Section 3.2 works.

A diagram of the process is shown in Figure 2. The process inputs are v_1 and v_2 (input voltages to the pumps). The experiments presented in this section consider only the analytical redundancy

DOI: 10.1002/acs

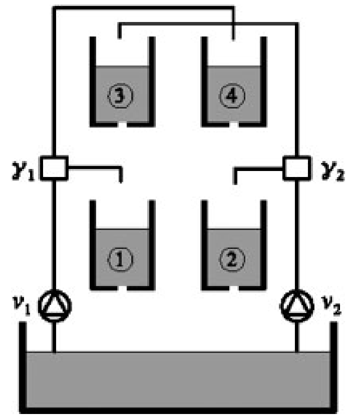

Figure 2. Quadruple-tank process.

relation coming from the first tank assuming that levels h_1, h_3 and voltage v_1 are measured

$$\frac{\mathrm{d}h_1}{\mathrm{d}t} = -\frac{a_1}{A_1}\sqrt{2gh_1} + \frac{a_3}{A_1}\sqrt{2gh_3} + \frac{\gamma_1 k_1}{A_1} v_1 \tag{27}$$

where $A_1 = 28\,\mathrm{cm}^2$, $k_1 = 3.33\,\mathrm{cm}^3/\mathrm{V\,s}$ and $g = 981\,\mathrm{cm/s}^2$. Parameters a_1 and γ_1 are assumed to belong to the intervals $a_1 \in [-0.029, 0.171]$ and $\gamma_1 \in [0.55, 0.85]$. The fault detection algorithm is tested in three different cases of parametric fault scenarios affecting a_1 and γ_1. For all cases the non-faulty system is simulated with parameters equal to $a_1 = a_3 = 0.071\,\mathrm{cm}^2$, $a_2 = a_4 = 0.057\,\mathrm{cm}^2$, $\gamma_1 = 0.7$ and $\gamma_2 = 0.6$.

Equation (27) can be expressed in the form given by Equation (1), once Euler discretization with sampling time equal to 1 has been applied

$$h_1(k+1) = h_1(k) + \left(-\frac{a_1}{A_1}\sqrt{2gh_1(k)} + \frac{a_3}{A_1}\sqrt{2gh_3(k)} + \frac{\gamma_1 k_1}{A_1} v_1(k) \right) + e_1(k) \tag{28}$$

where $|e_1(k)| \leqslant 0.02$ is a bounded random noise. Note that the results obtained in this section could be improved using the other three equations of the model. Considering that the parameter vector θ is composed of $\theta = [a_1 \; a_3 \; \gamma_1]^{\mathrm{T}}$, the regressor vector can be expressed as follows:

$$\varphi_{y_1}(k) = \left[-\frac{\sqrt{2gh_1(k)}}{A_1} \; \frac{\sqrt{2gh_3(k)}}{A_1} \; \frac{k_1 v_1(k)}{A_1} \right]^{\mathrm{T}} \tag{29}$$

Taking the uncertainty intervals associated with a_1 and γ_1 given above into account, the initial parameter uncertainty set for the fault detection stage is assumed to be

$$\Theta = \{\theta : \theta = p_0 + H_0 \tilde{\theta}, \; \|\tilde{\theta}\|_\infty \leqslant 1\}$$

where $p_0 = [0.071 \; 0.071 \; 0.7]^{\mathrm{T}}$, $H_0 = \mathrm{diag}([0.1 \; 0 \; 0.15]^{\mathrm{T}})$.

DOI: 10.1002/acs

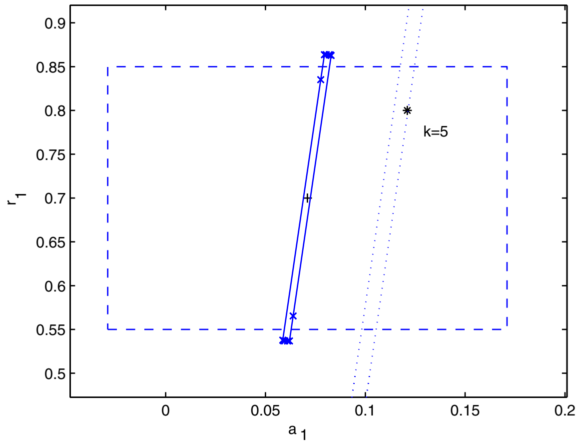

Figure 3. Fault detection test for time-invariant case, a_1 *vs* γ_1.

6.1. *Time-invariant parameters*

First, uncertain parameters are considered time invariant, that is, $\lambda = 0$ in Equation (4). The fault considered is a variation in the parameters a_1 and γ_1 from time instant $k = 5$: $a_{1f} = a_1 + 0.05$ and $\gamma_{1f} = \gamma_1 + 0.1$. This variation of parameters is inside the initial zonotope, but as the parameters are assumed to be invariant a fault should be indicated. Figure 3 shows the result of the fault detection test. The dashed box represents the initial zonotope for a_1 and γ_1. The solid line represents the zonotope intersection of the parameters consistent with the first four measurement outputs. The dotted line represents the band of parameters consistent with the measurement output for time instant $k = 5$. As this band does not intersect with the zonotope, a fault is consequently indicated.

6.2. *Time-varying parameters case 1*

In this case, uncertain parameters are considered time varying with

$$\lambda = \mathrm{diag}([0.01\ 0\ 0.03]^{\mathrm{T}})$$

in Equation (4). The fault considered is a variation in the parameters a_1 and γ_1 from time instant $k = 5$: $a_{1f} = a_1 + 0.03$ and $\gamma_{1f} = \gamma_1 + 0.05$. Despite this variation, the parameters are inside their uncertainty intervals. However, as the variation is higher than the allowed value at each time instant given by λ, a fault should be indicated. Figure 4 shows the fault detection test at time instant $k = 5$. The dashed box represents the valid interval for parameters a_1 and γ_1. The solid lines represent the zonotope that bounds the parameters consistent with the first four measurement outputs. The dotted line represents the band of parameters consistent with the measurement output for time instant $k = 5$. As this band does not intersect with the zonotope, a fault is effectively indicated.

6.3. *Time-varying parameters case 2*

Finally, uncertain parameters are considered to be time varying with $\lambda = \infty$ in Equation (4). This means that the parameters are only by the initial parameter set Θ but they can vary within this set. The fault considered is outside the box of allowed parameters, from time instant $k = 5$, that

DOI: 10.1002/acs

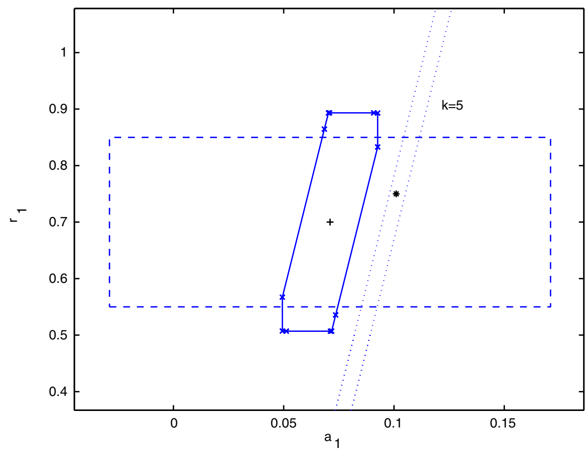

Figure 4. Fault detection test for time-varying case 1, a_1 *vs* γ_1.

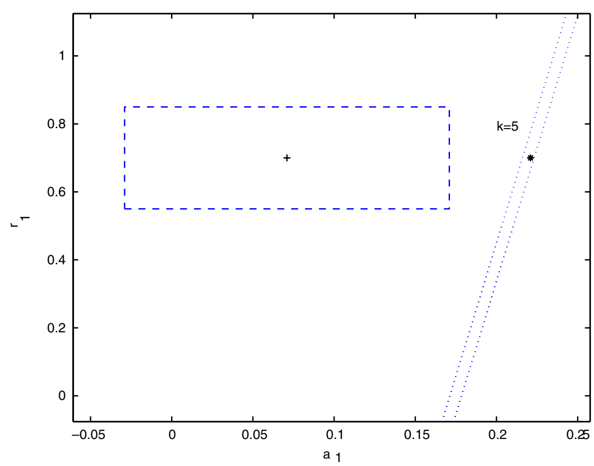

Figure 5. Fault detection test for time-varying case 2, a_1 *vs* γ_1.

is $a_{1f} = a_1 + 0.15$. Figure 5 shows the fault detection test result. The dashed box represents the allowable parameters region for a_1 and γ_1. The dotted line represents the band of parameters consistent with the measurement output for time instant $k = 5$. A fault is indicated as this band does not intersect with the box of allowed parameters.

7. APPLICATION EXAMPLE 2: SEWER NETWORK

As a second application example, the zonotope-based consistency approach for robust fault detection is tested on the limnimeters (water-level meters) of Barcelona's sewer system where they are used for the control system [22]. A telemetry network containing more than 100 limnimeters

DOI: 10.1002/acs

connected to a Supervisory Control and Data Acquisition system has been in operation since 1994. One of the main problems is that often these instruments are out of order in rain scenarios when the control system must be fully operative.

7.1. Limnimeter models

Limnimeters can be monitored using a rainfall-runoff model of the sewer network. Complex non-linear rainfall-runoff models are very useful for off-line operations (calibration and simulation) of the sewer network, but for online purposes (as for the global optimal control and fault detection and diagnosis), a more simpler structure of the model must be selected. One possible model methodology to derive a rainfall-runoff real-time model of a sewerage network is through a simplified graph relating the main sewers and set of virtual and real reservoirs [22]. A virtual reservoir is an aggregation of a catchment of the sewer network that approximates the hydraulics of rain, runoff and sewage water retention thereof. The hydraulics of virtual reservoirs are

$$\frac{\mathrm{d}V(t)}{\mathrm{d}t} = Q_{\mathrm{up}}(t) - Q_{\mathrm{down}}(t) + P(t)S \tag{30}$$

where V is the volume of water accumulated in the catchment, Q_{up} and Q_{down} are flows entering and exiting the catchment, P is the rain intensity falling in the catchment and S is its surface. Upstream L_{up} and downstream L_{down} sewer levels are measured using limnimeters and they can be related with flows using a linearized Manning relation

$$\begin{aligned} Q_{\mathrm{up}}(t) &= M_{\mathrm{up}} L_{\mathrm{up}}(t) \\ Q_{\mathrm{down}}(t) &= M_{\mathrm{down}} L_{\mathrm{down}}(t) \end{aligned} \tag{31}$$

where M_{up} and M_{down} are the Manning constants associated with upstream and downstream sewers.

Assuming that in Equation (30)

$$Q_{\mathrm{down}}(t) = K_v V(t) \tag{32}$$

substituting Equation (31) into Equation (30) and discretizing, we obtain

$$L_{\mathrm{down}}(k+1) = aL_{\mathrm{down}}(k) + bL_{\mathrm{up}}(k) + cP(k) \tag{33}$$

where $a = (1 - K_v \Delta t)$, $b = M_{\mathrm{up}} K_v \Delta t / M_{\mathrm{down}}$ and $c = SK_v / M_{\mathrm{down}}$.

Using this modeling methodology, a model of a part of the Barcelona's sewer network is presented in Figure 6. Its structure depends on the topology of the network and its parameters are estimated using the real data from the sensors in the network.

7.2. Zonotope-based consistency test (time-invariant case)

The zonotope-based consistency test for robust fault detection, described in Section 3.2, is applied to limnimeter L_{45} of the Barcelona's sewer network. According to the modeling methodology presented in the previous section and taking into account the conceptual scheme for the portion

DOI: 10.1002/acs

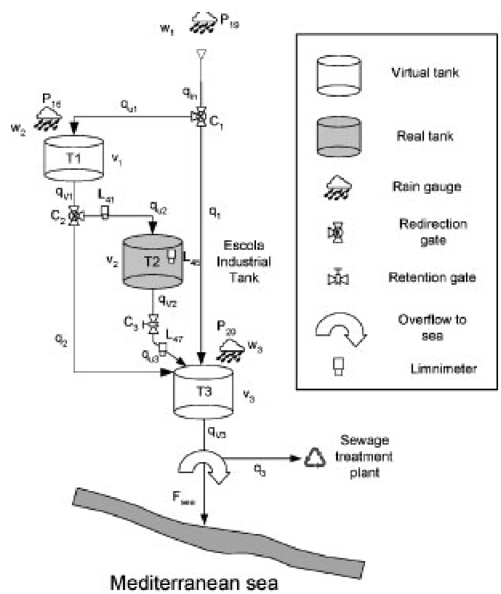

Figure 6. Virtual reservoir model of the Barcelona prototype network.

of sewer network considered (Figure 6), this limnimeter is related with limnimeters L_{41} and L_{47}. Its model can be represented by Equation (1) considering that

$$\begin{aligned} y(k) &= L_{45}(k) \\ \varphi(k) &= [L_{45}(k-1)\ L_{47}(k-1)\ L_{41}(k-1)] \\ \theta(k) &= [\theta_1(k)\ \theta_2(k)\ \theta_3(k)]^{\mathrm{T}} \end{aligned} \tag{34}$$

First, it will be assumed that parameters θ are time invariant (i.e. $\lambda=0$). Using a set of non-faulty scenarios (14/01/2001, 20/04/2001, 03/05/2001, 04/05/2001 and 05/05/2001) the feasible parameter set is estimated, adjusting measurement noise (σ) such that no fault is indicated.

Once the feasible parameter set has been estimated, it is used to initialize the fault detection algorithm (Algorithm 1) that is applied to the real faulty scenario 28/09/2001 provided by the Barcelona's sewer management company.

Figure 7 presents the result of the fault detection test. It can be observed that at time instant $k=6$ a fault is detected. Figure 8 presents the strip associated with the measurement data and the zonotope that approximates the feasible parameter set at this time. As the intersection is the empty set, this is why the fault is detected at that time (see Figure 7). It can also be noted that the strip associated with the measurement data is very wide. This is because the linear model for the liminimeter (33) is valid only around a given operating point. In fact, the real behavior is non-linear, which means the parameters of model (33) are not time invariant, but time varying according to the operating point. When considering those parameters as time invariant, parameter variance is implicitly considered as additive measurement noise to obtain a consistent model in the model identification phase. This forces to use a wide noise bound $\sigma=0.22$. According to the results presented in Section 5, this implies that fault detection test would require a bigger fault

DOI: 10.1002/acs

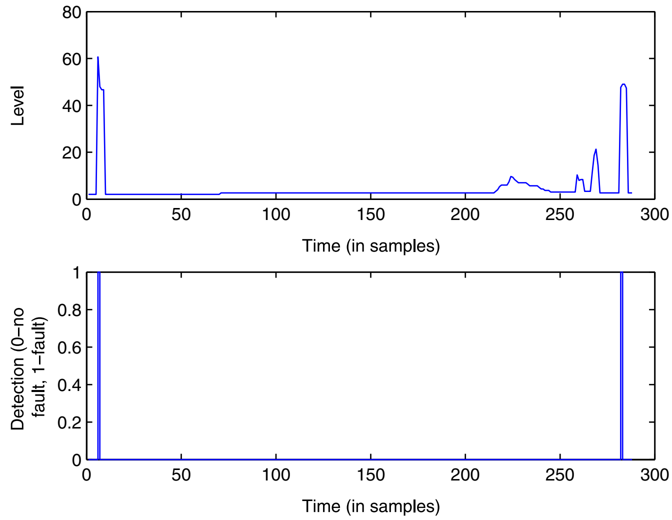

Figure 7. Result of detection test corresponding to episode 28/09/2001.

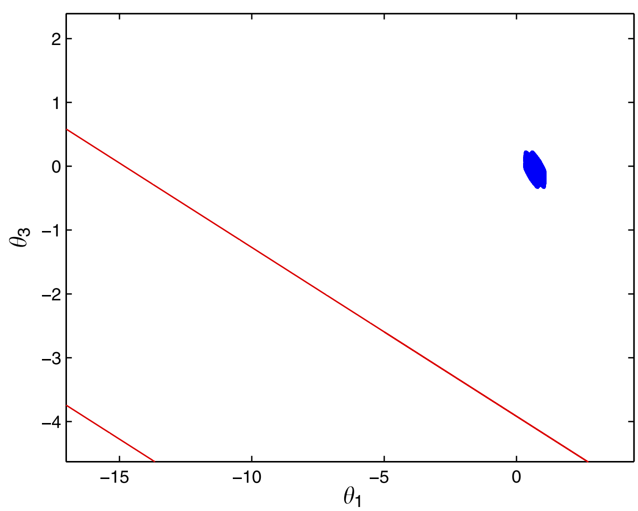

Figure 8. Intersection between strip and zonotope at time $k=6$ for episode 28/09/2001.

to be active as the minimum detectable depends on an inverse proportional way with respect to the noise bound σ. In order to decrease the size of the minimum detectable fault, noise bound could be reduced by taking into account parameter variance by considering that parameters are time varying with a bounded allowable variation instead of time invariant.

DOI: 10.1002/acs

7.3. Zonotope-based consistency test (time-varying case)

The allowed variance of parameters $\lambda(k)$ should also be estimated from real data coming from non-faulty scenarios. The procedure presented in Section 5.2 is used. Figure 9 shows how the maximum allowed parameters' variation (λ) varies when changing the measurement noise bound (σ), that is, there is a trade-off between measurement noise and allowed parameter variance bounds. Decreasing the measurement noise bound (in order to decrease the size of the minimum detectable fault) implies that the allowable parameter variance bound should be increased. Therefore, fixing the size of the minimum detectable fault, the required measurement noise bound can be determined. In particular, in the following, the noise bound has been set to $\sigma=0.16$, which leads to set the allowed parameter variance to $\lambda=\text{diag}([0.09\ 0.09\ 0.09]^{\mathrm{T}})$. This value has been determined using

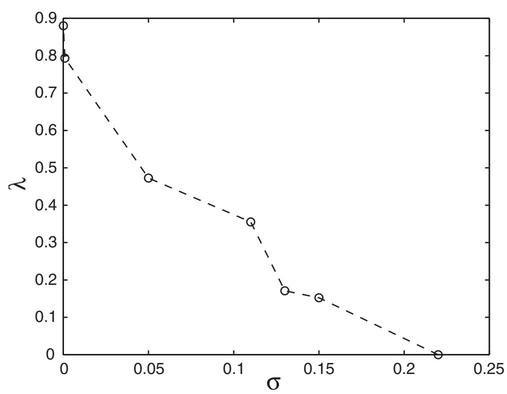

Figure 9. Allowed parameter variance (λ) *vs* measurement noise bound (σ).

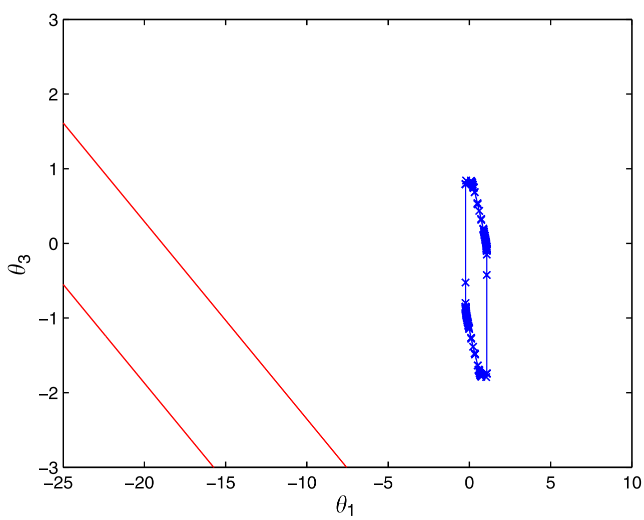

Figure 10. Intersection between strip and zonotope at time $k=6$ for episode 28/09/2001.

DOI: 10.1002/acs

Algorithm 2 in the parameter estimation phase in order to obtain a consistent model in case of the set of non-faulty scenarios considered (14/01/2001, 20/04/2001, 03/05/2001, 04/05/2001 and 05/05/2001).

Once the maximum allowed parameter variation has been estimated, fault detection using the conditional updating presented in Section 5.3 is used. The real faulty scenario 28/09/2001, already considered in Section 7.2 when parameters are assumed to be time invariant, is considered. Figure 10 presents the strip and the zonotope that approximates FPS at time $k = 6$ for the considered fault scenario. As the intersection is an empty set, the fault is detected. However, comparing with Figure 10, it can be seen that the strip is tighter as the noise bound is smaller, but the zonotope that approximates FPS is wider because of their expansion with the maximum allowed variation bound. This will allow one to detect smaller additive faults than in the case of considering parameters as time invariant.

8. CONCLUSIONS

A robust fault detection method has been proposed that takes advantage of a recently proposed set-membership identification procedure based on zonotopes for systems linear in the parameters. A general algorithm was presented based on proving that the feasible solution set of parameters for a series of data is empty. Three distinct cases of allowed parameter variance have been considered. Computational procedures based on zonotopes were given for each step in the algorithm and the minimum abrupt sensor and parametric fault detectable is characterized. Finally, the method was applied to two application examples: a four-tank system and a real application case (a piece of a sewer network) showing its effectiveness.

ACKNOWLEDGEMENTS

We thank the anonymous reviewers for their constructive comments and suggestions to improve this article. This work is supported by the Research Commission of the Generalitat of Catalunya (Grup SAC ref. 2005SGR00537) and by the Spanish Ministry of Science and Technology under grants DPI-2005-05415, DPI2006-15476-C02-01 and DPI2007-66718-C04-01.

REFERENCES

1. Chen J, Patton R. *Robust Model-based Fault Diagnosis for Dynamic Systems*. Kluwer Academic Publishers: Dordrecht, 1999.
2. Puig V, Quevedo J, Escobet T, Heras SDL. Robust fault detection approaches using interval models. *Proceedings IFAC World Congress* (*b'00*), Barcelona, Spain, 2002.
3. Fagarasan I, Ploix S, Gentil S. Causal fault detection and isolation based on a set-membership approach. *Automatica* 2004; **40**:2099–2110.
4. Armengol J, Trave-Massuyes L, Vehi J, de la Rosa JL. A survey on interval model simulators and their properties related to fault detection. *Annual Reviews in Control* 2000; **24**:31–39.
5. Puig V, Mrugalski M, Ingimundarson A, Quevedo J, Witczak M, Korbicz J. A gmdh neural network based approach to passive robust fault detection using a constraints satisfaction backward test. *IFAC World Congress*, Prague, Tzech Republic, 2005.
6. Fogel E, Huang YF. On the value of information in system identification—bounded noise case. *Automatica* 1982; **18**:229–238.
7. Pearson RK. Block-sequential algorithms for set-theoretic estimation. *SIAM Journal on Matrix Analysis and Applications* 1988; **9**:513–527.

8. Vicino A, Zappa G. Sequential approximation of feasible parameter sets for identification with set membership uncertainty. *IEEE Transactions on Automatic Control* 1996; **41**:774–785.
9. Watkins J, Yurkovich S. Fault detection using set-membership identification. *IFAC World Congress*, San Francisco, U.S.A., 1996.
10. Lesecq A, Barraud K, Dhin T. Numerical accurate computations for ellipsoidal state bounding. *Eleventh Mediterranean Conference on Control and Automation MED'03*, Rhodes, Greece, 18–20 June 2003.
11. Tzes A, Le K. Fault detection for jump discrete systems. *IEEE Proceedings of the American Control Conference*, San Diego, U.S.A., 1999.
12. Kesavan P, Lee JH. A set based approach to detection and isolation of faults in multivariable systems. *Computers and Chemical Engineering* 2001; **25**:925–940.
13. Chisci L, Garulli A, Vicino A, Zappa G. Block recursive parallelotopic bounding in set membership identification. *Automatica* 1998; **34**:15–22.
14. Bravo JM, Alamo T, Camacho EF. Bounded error identification of systems with time-varying parameters. *IEEE Transactions on Automatic Control* 2006; **51**:1144–1150.
15. Combastel C, Zhang Q. Robust fault diagnosis based on adaptive estimation and set-membership computations. *Proceedings of SAFEPROCESS 2006*, Beijing, China, 2006.
16. Ploix S, Adrot O. Parity relations for linear uncertain dynamic systems. *Automatica* 2006; **42**:1553–1562.
17. Blanke M, Kinnaert M, Lunze J, Staroswiecki M. *Diagnosis and Fault-tolerant Control*. Springer: Berlin, Heidelberg, 2003.
18. Gertler J. *Fault Detection and Diagnosis in Engineering Systems*. Marcel Dekker: New York, 1998.
19. Nyberg M, Krysander M. Combining ai, fdi and statistical hypothesis-testing in a framework for diagnosis. *Proceedings of IFAC Safeprocess'03*, Washington, U.S.A., 2003; 891–896.
20. Isermann R. Process fault detection based on modelling and estimation methods. *Automatica* 1984; **20**:387–404.
21. Johansson KH, Nunes JLR. A multivariable laboratory process with an adjustable zero. *Proceedings of 17th American Control Conference*, Philadelphia, PA, 1998.
22. Cembrano G, Quevedo J, Salamero M, Puig V, Figueras J, Mart J. Optimal control of urban drainage systems: a case study. *Control Engineering Practice* 2004; **12**(1):1–9.

DOI: 10.1002/acs